Springer

Journal of
Mechanical
Science and
Technology

Journal of Mechanical Science and Technology 22 (2008) 190~200

www.springerlink.com/content/1738-494x

A study on impulsive sound attenuation for a high-pressure blast flowfield

Kuk-Jeong Kang[1,*], Sung-Ho Ko[2] and Dong-Soo Lee[3]

[1]*Senior Researcher, Ground System Development Center, Agency for Defence Development, 215 Sunam-dong, Yuseong-gu, Daejeon, 305-600, Korea*

[2]*Prof., Department of Mechanical Design Engineering, Chungnam National University, 220 Gung-dong, Yuseong-gu, Daejeon, 305-764, Korea*

[3]*Student, Department of Mechanical Design Engineering, Chungnam National University, 220 Gung-dong, Yuseong-gu, Daejeon, 305-764, Korea*

(Manuscript Received December 29, 2006; Revised April 21, 2007; Accepted July 25, 2007)

Abstract

The present work addresses a numerical study on impulsive sound attenuation for a complex high-pressure blast flowfield; these characteristics are generated by a supersonic propellant gas flow through a shock tube into an ambient environment. A numerical solver for analyzing the high pressure blast flowfield is developed in this study. From numerical simulations, wave dynamic processes (which include a first precursor shock wave, a second main propellant shock wave, and interactions in the muzzle blasts) are simulated and discussed. The pressure variation of the blast flowfield is analyzed to evaluate the effect of a silencer. A live firing test is also performed to evaluate four different silencers. The results of this study will be helpful in understanding blast wave and in designing silencers.

Keywords: Blast wave; Impulsive noise; Silencer; Live firing test

1. Introduction

When a gun fires, excessive noise is created in the form of a blast wave. As the muzzle energy of the weapon system increases, the level of impulsive noise also increases. It is well known that the impulsive noise from a gun may seriously damage human bodies and structures. An investigation of the noise levels at various distances from the test site showed that the gun firings could be heard ten miles away at a level of 90 dB. Impulsive sound may also cause both social and military problems. Thus, the study of blast wave and impulsive sound attenuation is of great importance.

An impulsive sound has several different properties compared to continuous noise. These special features are high energy, impulsiveness, low frequency, strong directivity, and long range propagation. Firing noises can be divided into three categories: muzzle blast, projectile noise, and noise of explosion of the projectile at the target (Fig. 1). The first and second of these are strongly directional. Low-frequency components dominate all three blasts that propagate over distances of several kilometers, yielding significantly high noise levels.

A muzzle blast is produced by a propellant explosion inside a gun barrel. The deflagration of a propellant in a chamber produces an abrupt expansion of gases. This rapid increase in volume causes pressure waves which accelerate the projectile into flight. It can be heard as a muzzle blast.

The muzzle blast has two main properties that differentiate it from common environmental noise: short duration and high amplitude. The sound waves, especially near the emplacement, are short and impulsive. The duration of the impulse is generally only of the

*Corresponding author. Tel.: +82 42 821 2541
E-mail address: kshsj85@hanafos.com
DOI 10.1007/s12206-007-1023-8

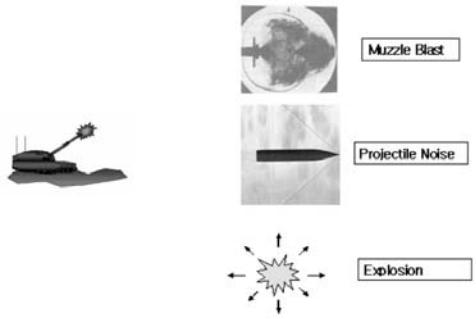

Fig. 1. Schematic configuration of the sound generation and the propagation.

order of milliseconds close to the source. For small caliber weapon systems (SCWS) the positive pulse duration can be less than 0.5 milliseconds and for large caliber weapon systems (LCWS) it can be a few milliseconds.

Another type of firing noise is produced by a projectile. The most prominent trait of projectile noise is the sonic boom. Because the leading overpressure cannot avoid the projectile, due to its supersonic speed, the sound wave becomes a conically expanding shock wave.

Impact noise is generated by a collision of the projectile into a target. For SCWS this is of low importance but for LCWS this can produce the predominant portion of the firing noise.

The suppression of the muzzle blast is important in both LCWS and SCWS designs. In the case of LCWS, the primary objective of overpressure attenuation is to reduce the blast on structures, operating crews, and supporting vehicles. The design of silencer has relied heavily on experimental work and the development of empirical databases.

The research on impulsive noise is divided into two categories: noise attenuation and blast wave analysis. In Korea there has been no research on impulsive noise attenuation. Several countries, such as the U.S. and Germany, also have impulsive noise problems; they have continually investigated impulsive sound attenuation. However, they haven't seemed to have found an effective solution to the problem yet.

In the 1980s, the German Ministry of Defence (MoD) launched a research program [1, 2] on military shooting noise. The first steps of this program were to measure shooting sounds produced in facilities, to set up a blast propagation model, and to conduct surveys in order to design an objective assessment scheme for shooting noise. After this, steps were taken to determine what additional information was needed to predict and assess shooting noise in the vicinity of complex installations. The goal of this program was only to develop a blast propagation model and to construct a management scheme for shooting noise. Research on the attenuation of impulsive firing noise was not considered.

The Noise Prognosis Model [3] was developed for the production of Noise Maps (LARMLAST). This program requires a database indicating firing locations, type and frequency of firing, and also noise propagation data for the weapons. The maps serve as a planning basis for the layout of firing ranges, for the construction of noise abatement structures directly at the source, and for noise protection measures to be taken at residential areas. A suitable sound absorbing structure for low-frequency pulse-type noise was designed; it yields a noise reduction of about 10 dB. It also offers restrictive firing for LCWS and has a massive scale. It seems that the noise attenuation of this program is confined to low levels and, as well, details of the design parameters of structures were not presented.

Alternatively, BRL [4] designed a noise attenuator to be used with the tank cannon proofing work to reduce the propagation of gun firing noise from Aberden Proving Ground to the surrounding community [5]. The location of the muffler baffles and overall sizing were determined through configurable muffler experiments and computer modeling. But this noise attenuator had serious structural weaknesses and noise attenuation was minimal.

There was also a numerical study which focused on wave dynamic processes occurrng in muzzle blast flows; these wave dynamic processes are created by supersonic projectile releases from the open-end of a shock tube into ambient air [6]. Using numerical simulations, wave dynamic processes including two blast waves, two jet flows, the bow shock wave, and their interactions in the muzzle blasts are demonstrated and discussed. The study shows that the major wave dynamic processes developing in the muzzle flow remain similar when the friction varies, but that some wave processes such as shock-shock interactions, shock-jet interactions, and contact surface instability, become more intensive, resulting in more complex muzzle blast flows. In only two cases the pressure ratio (1.25 and 1.75) behind the projectile and ahead of the projectile was analyzed. An investigation of a higher pressure ratio is needed to study the

influences of wave dynamic processes and wave interactions for LCWS.

In another study, computational fluid dynamic methods were considered and evaluated for designing muzzle blast suppressors for firearms [7]. This study summarizes an initial experimental and computational investigation into suppressors for 0.22 caliber/5.56 mm and 0.38 caliber/9 mm guns. These simulations correctly capture both the levels and characteristics of the acoustic signal generated by the bare muzzle and suppressor configurations. Discrepancies were taken into account by assuming a constant projectile velocity. A limitation of this research is that it focused mainly on SCWS.

The main purpose of the present study was to perform experimental and numerical analyses on impulsive sound attenuation in a high-pressure blast flowfield. The supersonic blast flowfield was analyzed to evaluate the noise attenuation of a silencer. The gun was modelled as a shock tube to simulate a gun's blast wave. Then, numerical analysis was performed for the cases that a silencer was installed to the muzzle. Next, live firing tests were performed to evaluate the silencer through experimental methods.

2. Numerical analysis

2.1 Governing equation

The governing equations for the three-dimensional, unsteady, compressible, and turbulent flow of the gun blast can be written as Reynolds averaged Navier-Stokes equations. These equations can be transformed into a curvi-linear coordinates system as follows:

$$\partial_\tau \hat{Q} + \partial_\xi \hat{E} + \partial_\eta \hat{F} + \partial_\zeta \hat{G} = \partial_\xi \hat{M} + \partial_\eta \hat{N} + \partial_\zeta \hat{P} \qquad (1)$$

where $\hat{Q}, \hat{E}, \hat{F}$ and $\hat{G}$ denote the dependent variables and the flux vectors, respectively, given by

$$\hat{Q} = \frac{1}{J}\begin{bmatrix} \rho \\ \rho u \\ \rho v \\ \rho w \\ e \end{bmatrix}, \hat{E} = \frac{1}{J}\begin{bmatrix} \rho U \\ \rho uU + \xi_x p \\ \rho vU + \xi_y p \\ \rho wU + \xi_z p \\ UH - \xi_t p \end{bmatrix},$$
$$\hat{F} = \frac{1}{J}\begin{bmatrix} \rho V \\ \rho uV + \eta_x p \\ \rho vV + \eta_y p \\ \rho wV + \eta_z p \\ VH - \eta_t p \end{bmatrix}, \hat{G} = \frac{1}{J}\begin{bmatrix} \rho W \\ \rho uW + \zeta_x p \\ \rho vW + \zeta_y p \\ \rho wW + \zeta_t p \\ WH - \zeta_t p \end{bmatrix} \qquad (2)$$

where ρ is density, u, v, w are cartesian velocity components for the x, y, z directions, respectively, p is the pressure, e is the total energy per unit volume, ξ_x, ξ_y, ξ_z are the coordinate transformation metrics, and J is the coordinate transformation Jacobian, H is enthalpy, U, V, W are the contravariant veloc ity components. $\hat{M}, \hat{N}, \hat{P}$ terms denote the viscous terms and can be described using tensor notation as follows:

$$\hat{M} = \frac{1}{J}\begin{bmatrix} 0 \\ \xi_i \tau_{xi} \\ \xi_i \tau_{yi} \\ \xi_i \tau_{zi} \\ \xi_i \beta_i \end{bmatrix}, \hat{E} = \frac{1}{J}\begin{bmatrix} 0 \\ \eta_i \tau_{xi} \\ \eta_i \tau_{yi} \\ \eta_i \tau_{zi} \\ \eta_i \beta_i \end{bmatrix}, \hat{F} = \frac{1}{J}\begin{bmatrix} 0 \\ \zeta_i \tau_{xi} \\ \zeta_i \tau_{yi} \\ \zeta_i \tau_{zi} \\ \zeta_i \beta_i \end{bmatrix} \qquad (3)$$

Here β_i can be described as $\beta_i = u_j \tau_{ij} - q_i$, shear stress τ can be expressed by laminar viscous coefficient μ and eddy viscous coefficient μ_t:

$$\tau_{ij} = (\mu + \mu_t)[(\frac{\partial u_i}{\partial x_j} + \frac{\partial u_j}{\partial x_i}) - \frac{2}{3}\delta_{ij}\frac{\partial u_k}{\partial x_k}] \qquad (4)$$

From the ideal gas state equation, the pressure p is given by

$$p = (\gamma - 1)[e - \frac{\rho}{2}(u^2 + v^2 + w^2)] \qquad (5)$$

2.2 Numerical analysis method

A finite difference code based on computational fluid dynamics was developed to analyze the supersonic blast flowfield and to design gun silencers. This numerical solver uses Roe's upwind scheme as a spatial derivative and a second order central scheme for viscous terms. The LU-SGS implicit scheme is used for time integration and the Baldwin-Lomax turbulence model is used. Additionally, the multi-block grid technique is applied to analyze the complicated geometry of the gun muzzle. The grid points in overlapped regions are constructed so as to exactly coincide and to preserve the conservations of fluxes across the grids.

Initially, the internal portion of the gun barrel was filled with gases of high pressure and high temperature. The shock wave is located at the muzzle exit. The viscous (no-slip) adiabatic wall boundary condition is applied. At inflow and outflow boundaries, a

characteristic boundary condition is applied, which is based on the Riemann invariants.

3. Numerical simulations

3.1 Verification of numerical solver

The appropriateness of the numerical solver for analyzing the supersonic flowfield can be validated through solving the shock tube problem. This problem was tested by Schmidt and Duffy and quoted in a paper by Wang and Widhopf [8]. Schmidt and Duffy investigated the blast flowfield using an open cylindrical shock tube (Fig. 2). In their shock tube experiment, the pressure around the muzzle was measured for the pressure ratio 3.42. Thus the same domain was selected for verifying the numerical solver.

Fig. 2 shows a schematic diagram of the computational domain. The calculation was started by placing a shock of strength $M_s = 1.76$ and $p_2 / p_1 = 3.42$ at the exit. The points at which the data was measured are represented in Fig. 2. Fig. 3 shows a comparison between the experimental [8] and computational results of the pressure time histories at the positions x/D=0.0125, z/D=1.49 and x/D=0.738, z/D=1.29.

The wave arrival, the rise time, and the peak pressure value at each measurement location agree well with numerical results produced by the current numerical solver. As well, good agreement with measured pressure time histories was obtained. These processes demonstrate the appropriateness and suitability of the numerical solver for analyzing the supersonic blast flowfield.

3.2 High pressure blast flowfield analysis without silencer

Before investigating a high pressure blast flowfield with a silencer, it is necessary to analyze the supersonic blast flowfield in which a silencer is not installed on the gun muzzle. These results will then be compared with the results in which a silencer is used. Fig. 4 shows a schematic diagram of the computational domain, and the initial and boundary conditions. At the initial frame, the shock wave arrives at the exit of the shock tube. Here the pressure ratio between

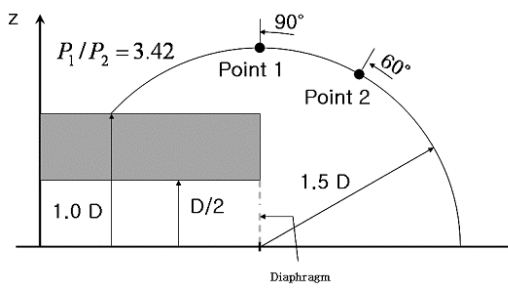

Fig. 2. Schematic diagram of the computational domain (low pressure shock tube).

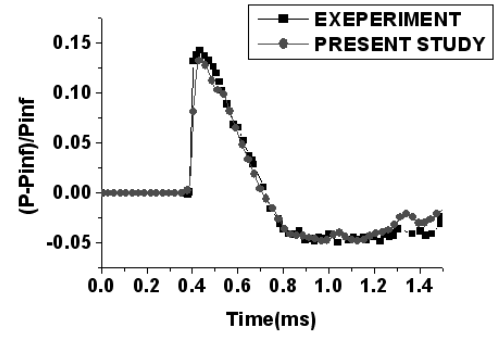

(a) x/D=0.0125, z/D=1.49(point 1)

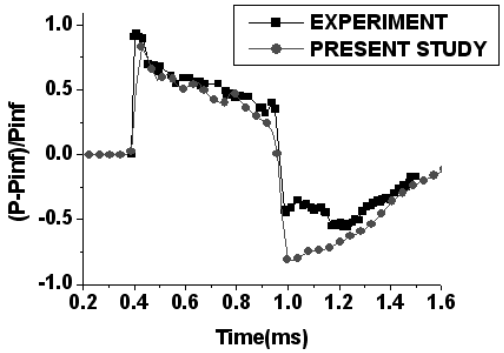

(b) x/D=0.738, z/D=1.29((point 2)

Fig. 3. Comparison between the experimental and computational results.

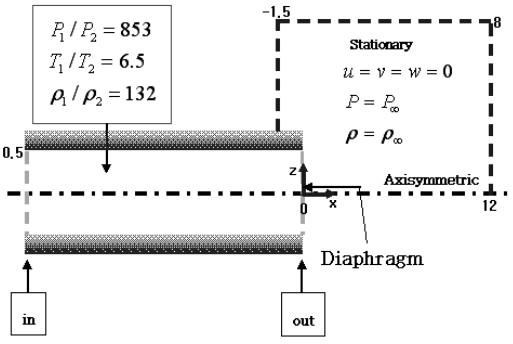

Fig. 4. Schematic diagram of the computational domain (high pressure blast flowfield).

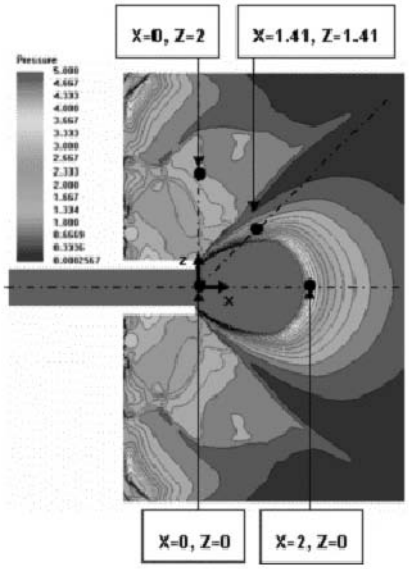

Fig. 5. Data points for pressure calculation in front of the muzzle exit region.

high and low pressure sections is 853. The density and the temperature ratios are 132 and 6.5, respec tively. The surrounding condition is ambient air of $P = P_\infty$, $\rho = \rho_\infty$.

Fig. 5 shows the data points for pressure calculation in front of the muzzle exit. A round plume boundary is shown at the front of barrel, and an oblique shock and a Mach disk are located in front of the muzzle. The formation of a contact surface between the high pressure propellant gas region and the low pressure air region is presented.

Fig. 6(a) shows the pressure variation at the exit of the gun muzzle (X=0, Z=0). Through the interactions of shock wave, continuous expansion and reflection of muzzle flow, reflected shock and strong pressure fluctuation is expected. Furthermore, the pressure ratio between high and low pressure sections is very high (853). For these reasons, a sharper shock front may be investigated at the exit region of the gun muzzle. Fig. 6(b) shows the pressure variation occurring at the front of the muzzle exit (X=2, Z=0). At the outer region of the Mach disk, the pressure is diminished by the expansion of the propellant gases and the pressure is decreased to 166. Fig. 6(c) and 6 (d) show the pressure at the upper region of the gun muzzle. It is interesting to note that the pressure of the upper region has a lower value than that of the frontal region. It is evident that the supersonic blast flowfield mainly affects the frontal area. The present data shows that

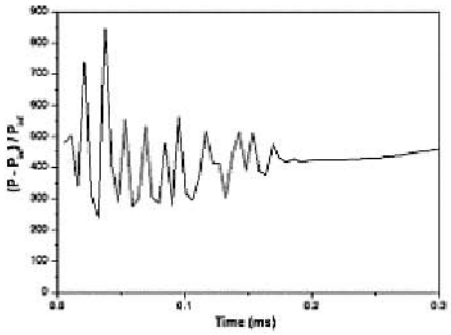

(a) Pressure variation at X–0, Z–0

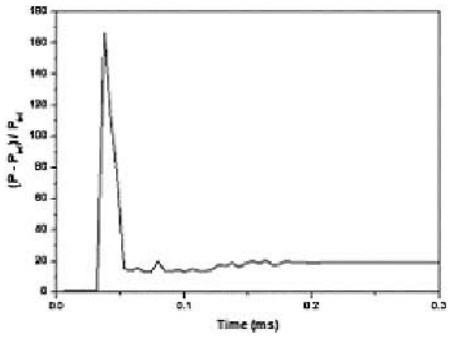

(b) Pressure variation at X–2, Z–0

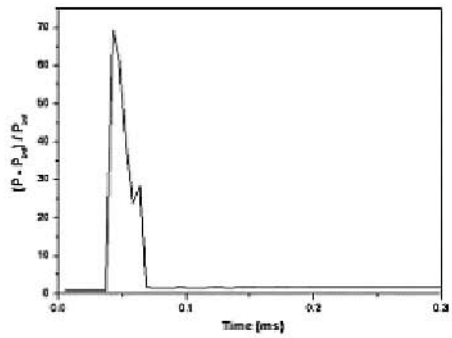

(c) Pressure variation at X–1.414, Z–1.414

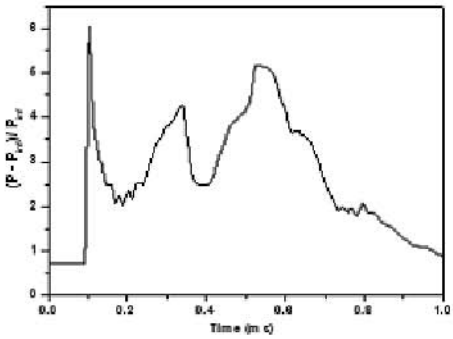

(d) Pressure variation at X=0, Z=2

Fig. 6. Pressure in front of the muzzle exit.

strong fluctuation of the pressure mainly occurs at the muzzle exit. It is also clear that the pressure in the longitudinal direction is significantly high and has a dominant role in generating the firing noise.

3.3 High pressure blast flowfield analysis with silencer

The supersonic blast flowfield of a silencer which has three baffles is analyzed. Fig. 7 shows the configuration of the computational domain; it is comprised of 12 blocks and 1,500,000 cells, and the gun muzzle is enveloped by the silencer. The expansion volume of the silencer is extended to behind of the muzzle to maximize the attenuation. The first baffle, which receives the maximum pressure, should be designed to tolerate a firing load. Thus it has a thickness of 0.63 (x/D). The other baffles have a thickness of 0.38 (x/D).

The pressure ratio between the high and low pressure sections is 853, and the density and the temperature ratios are 132 and 6.5, respectively. The initial conditions are set using the results of an internal ballistic analysis.

Fig. 8 shows the predicted results for a blast wave formation in the near field of the exit. As the propellant gases pass through the baffles, continuous formation of a precursor shock wave and a propellant shock wave can be considered. The pressure of the main propellant shock wave is much higher than that of the precursor shock wave.

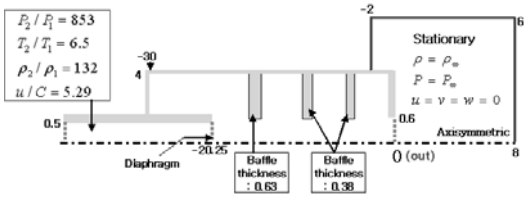

Fig. 7. Schematic diagram of the computational domain (silencer).

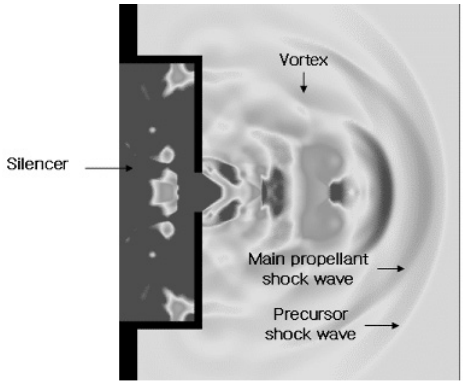

Fig. 8. Blast wave formation in the near field of the silencer exit.

Fig. 9 shows data acquisition points in the silencer, including the muzzle exit and the internal center line of each baffle. Through using the computational fluid dynamic scheme, the pressure of the silencer's internal region can be considered. The internal pressure of the silencer is calculated to consider the features of the blast flowfield. It is interesting to note that the pressure of the silencer decreases as the exit region is approached. This is due to the fact that propellant gases are dissipated in the chamber volumes. Through these processes, the pressure of the exit is much lower than that of the gun muzzle.

Fig. 10 shows the predicted results of pressure and sound pressure level at the inner regions of the silencer. These flow patterns are more complicated than with the simple silencer. The repetitive expansion and the reflection of the high pressure blast field are also calculated. Figs. 10(a), (b), (c), (d), and (e) show the pressure at points 1 to 5. It is very likely that the maximum pressure is lowered almost 99%.

Fig. 10(a) shows the pressure variation at point 1. Through the influences of the propellant shock wave, the maximum pressure of the muzzle exit (point 1) is 139 MPa. After the excessive vibration of pressures, the pressure of point 1 reaches a constant level. Fig. 10(b) shows the pressure variation of point 2, which is the exit area of the silencer's second volume. This point represents a very strong vibration of pressure. Through the silencer's dissipation effect, the pressure is attenuated from 139 to 15 MPa. As gases pass through the baffles [Fig. 10(c), (d)], successive pressure reduction is predicted, and the repetitive expansion and reflection of the high pressure blast field is calculated. At point 5 [Fig. 10(e)], a very low pres-

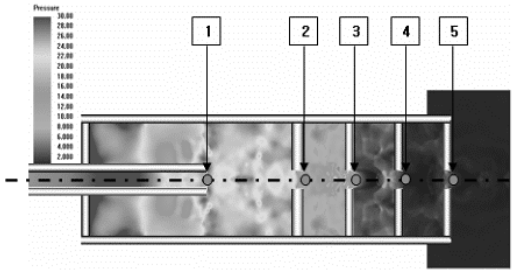

Fig. 9 Data acquisition points in the silencer.

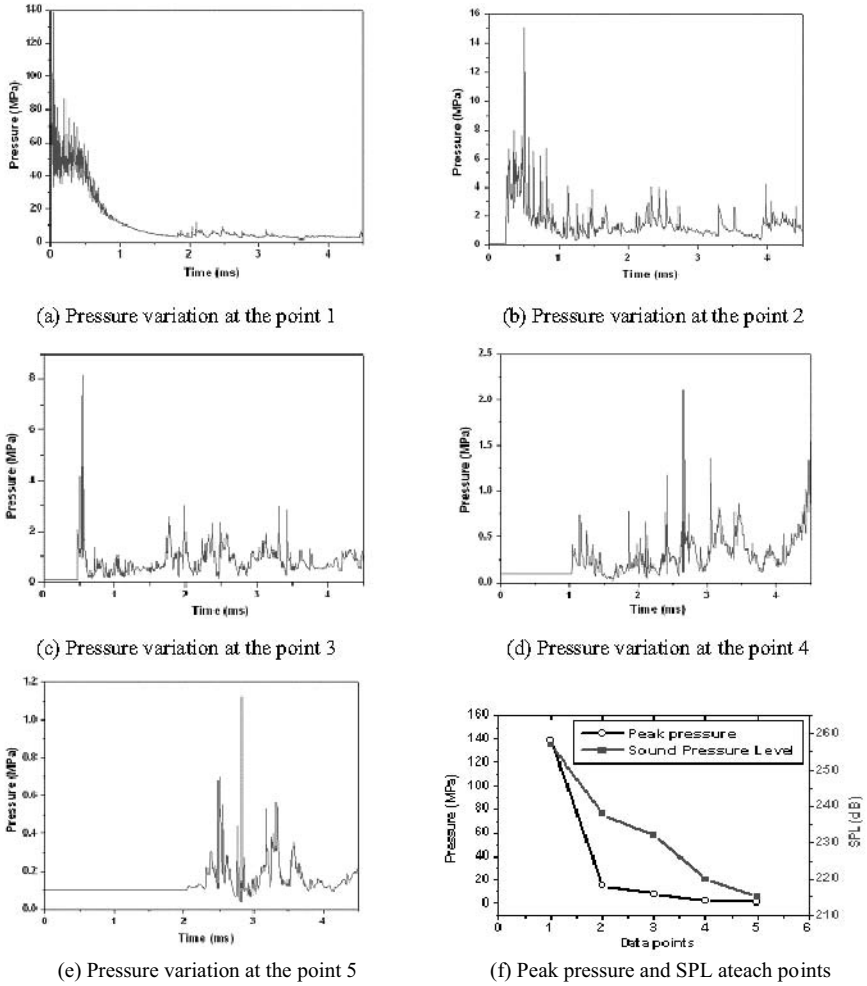

(a) Pressure variation at the point 1

(b) Pressure variation at the point 2

(c) Pressure variation at the point 3

(d) Pressure variation at the point 4

(e) Pressure variation at the point 5

(f) Peak pressure and SPL ateach points

Fig. 10. Predicted results of pressure and sound pressure level.

calculated. At point 5 (Fig. 10(e)), a very low pressure value of 1.1 MPa is calculated: the effect of the three baffle silencer in attenuating the sound pressure is expected. Fig. 10(f) represents the peak pressure and the sound pressure level relation in consideration of the attenuation of the silencer. At the exit region of the first baffle, the maximum attenuation can be anticipated through the effect of maximum volume in the first chamber, which has rearward regions. At the rearward region, the maximum pressure of the first volume occurs. The pressure between point 1 and point 5 decreases from 139 MPa to 1.1 MPa, and 99% of the pressure reduction is accomplished. The sound pressure level decreases from 257 to 215 dB. An almost 42 dB attenuation is predicted by the silencer.

Fig. 11 shows the predicted points of pressure in the ambient region, where the cases of r/D=2, 3, 4, and 6 are considered at the degree of 0 to 90. The energy of the blast wave ejected from the gun muzzle is diminished by the silencer.

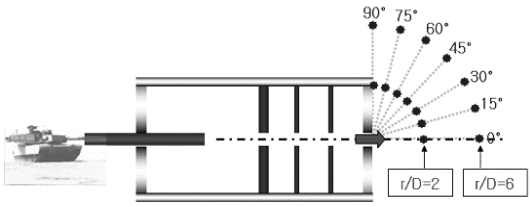

Fig. 11. Data points in the ambient region.

Fig. 12 shows the pressure variation of the ambient region in the positions r/D=2 and 4, respectively. The main portion of the firing energy is concentrated on the frontal region of the gun muzzle. Fig. 12 also shows a strong fluctuation in the pressure of the fron-

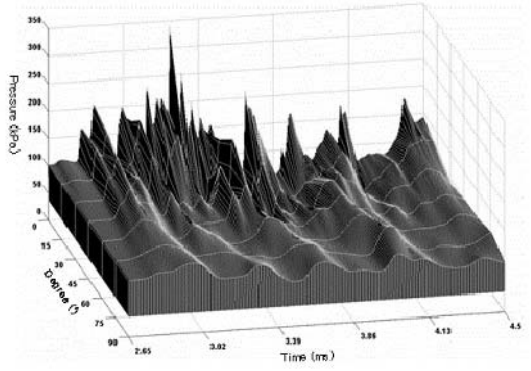

(a) Pressure variation at R/D=2

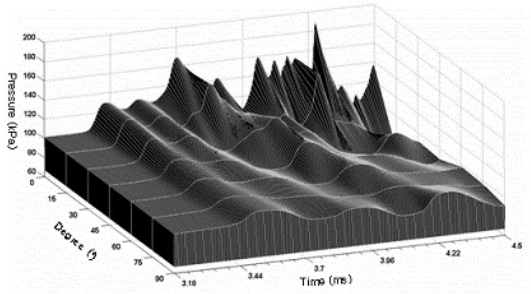

(b) Pressure variation at R/D=4

Fig. 12. Pressure variation of the ambient region.

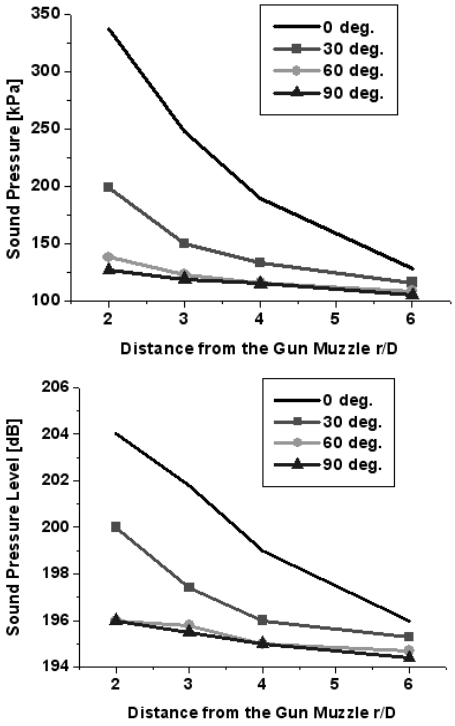

Fig. 13. Sound pressure and sound pressure level.

tal region. Through the silencer's dissipation of muzzle energy there is an almost 40 dB diminution of the sound pressure level.

Fig. 13 shows the sound pressure and the sound pressure level in the positions r/D=2, 3, 4, and 6, respectively. In all these cases, the pressure of the central area, which coincides with firing direction, is of a higher value. On the other hand, the pressure of the side area is of a lower value.

4. Live firing test

The blast flowfield for SCWS was analyzed to predict the performance of silencers. Four silencers were designed based upon numerical simulation. Then live firing tests for SCWS were performed to evaluate the attenuation of impulsive noise. Using LCWS for live firing tests would be unfeasible due to cost and other factors. Therefore, SCWS, which guarantee the similarity rule with LCWS in terms of Mach number, was adopted.

4.1 Design of silencer

The supersonic blast flowfield of silencer D and the bare muzzle was analyzed to predict exit pressure for the muzzle and the silencer. Fig. 14 shows the pressure at the exit of the muzzle and the silencer. From this result, the pressures of the exit were predicted at 850 and 7, respectively. In turn, it was expected that the silencer D would diminish almost 99% of the pressure. As well, it was estimated that a considerable amount of propellant energy would be dissipated by the silencer in the live firing test. Based upon these results, four silencers were designed. Fig. 15 shows the schematic configuration of the four silencers, which were made of aluminum.

4.2 Live firing test

The sound pressure was measured at distances of 2 and 4 m from the gun muzzle. The measuring angle was 90º from the firing direction to the right. To smooth the data plot, the Savitzky-Golay filter scheme, which is known to preserve features of data such as peak height and width, was used. The degree of the polynomial has a value of 2, with 23 points to a sound pressure and 51 points to a sound pressure level.

Fig. 16 represents the test results of measured

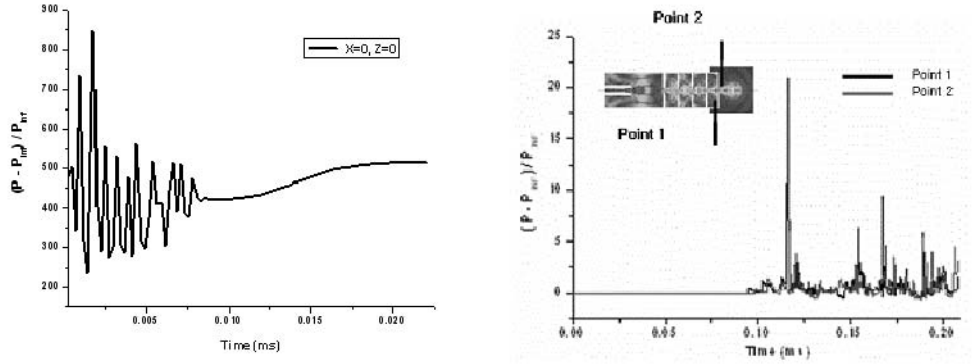

(a) Without silencer (b) With silencer D

Fig. 14. Calculation results of pressure at the exit of the muzzle and the silencer.

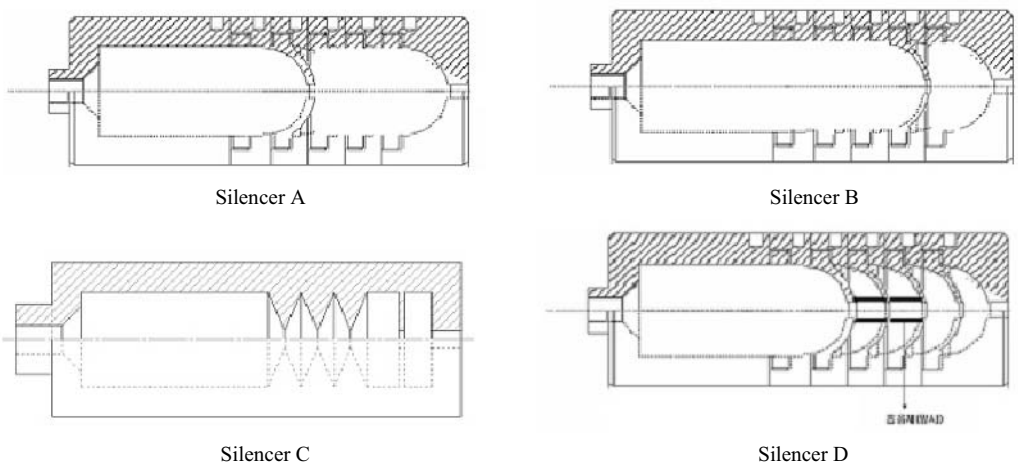

Fig. 15. Schemetic configuration of the four silencers.

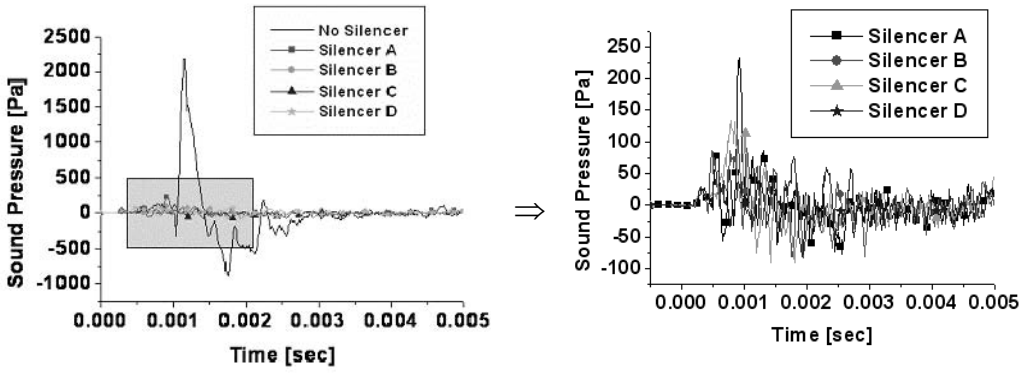

Fig. 16. Measured results of sound pressure.

sound pressure for the four silencers. With a bare muzzle, the peak pressure reaches 2,170 Pa. However for silencer A, the peak pressure decreases to a level of 232 Pa. Silencer A is characterized by two chambers with almost uniform volume. With the silencer, the occurrence of pressure is delayed for about 0.7 ms nd the quantity of firing energy is reduced. The present data shows that for the given silencers a consid-

erable amount of propellant energy is dissipated in the volume and that the sound pressure is diminished as well.

With silencer B, the peak pressure decreases to a level of 121 Pa. In silencer B, the first chamber has almost triple the volume of silencer A. Therefore, it is assumed that silencer B will better attenuate the firing sound pressure.

With silencer C, which has an attenuation feature similar to silencer B, the peak pressure decreases to a level of 134 Pa. Silencer C is characterized by four baffles arranged side by side. Because the propellant gas is expanded successively in a silencer, there is greater sound attenuation.

With silencer D, the peak pressure decreases to a level of 76 Pa. This is the best attenuation result of the four silencers. Silencer D is designed with four baffles arranged side by side, and the first chamber has the greatest volume. It also has two acoustic insulation materials in the flight passage to absorb and dissipate the firing sound pressure. Thus, the propellant gas expands and decreases successively in the silencer.

Fig. 17 represents the sound pressure at certain distances from the gun muzzle. At a distance of 2 m from the gun, the maximum pressure of the bare muzzle is 2,170 Pa, while the maximum pressure of the silencers decreases to below 80 Pa. In the case of silencer D, the attenuation ratio of sound pressure reached 97 %. Live firing test results show a similar trend for the diminution of pressure to the prediction results (Table 1). In the live firing test a similar diminution level of the exit pressure was confirmed.

At a distance of 4 m from the gun muzzle, similar sound pressure attenuation results were investigated. Additionally, in order to study noise influence, the sound pressure frequency should be investigated. Generally sound from 20 to 20,000 Hz can be heard; this is the audible frequency range. Therefore, for analyzing the firing sound pressure, the frequency range of 0 to 20 kHz is considered.

Table 1. Comparison between the live firing test results and the prediction results.

cases	unit	maximum pressure		remarks
		without silencer	with silencer	
live firing test (2 m from the muzzle)	[Pa]	2,170	76	97% reduction
prediction (muzzle exit)	-	850	7	99% reduction

Fig. 18 represents the sound pressure level according to frequency ranges for silencers. In the case of a bare muzzle, the sound pressure level reaches 165 dB at the low frequency range of below 2 kHz. But for silencer A, the sound pressure level were below 135 dB through all audible frequency ranges. At the range of 15 to 20 kHz, the sound pressure level reaches 125 dB and no attenuation is expected. Especially at the lower frequency ranges (under 10 kHz) noise attenuation is expected. But over the ranges of 10 to 20 kHz, silencer A does not effectively attenuate noise. It was found that silencer A achieves noise attenuation under the frequency range of 10 kHz.

In the case of silencer B, the sound pressure level decreases below 130 dB over the all audible frequency ranges. It achieves a 35 dB reduction of sound pressure level at low frequency ranges. In the case of silencer C, the sound pressure level reaches a maximum of 125 dB over all audible frequency ranges. It achieves a 40 dB reduction of sound pressure level at low frequency ranges. While silencer C generally achieves proper noise attenuation, over the range of 15 to 20 kHz it does not achieve noise attenuation.

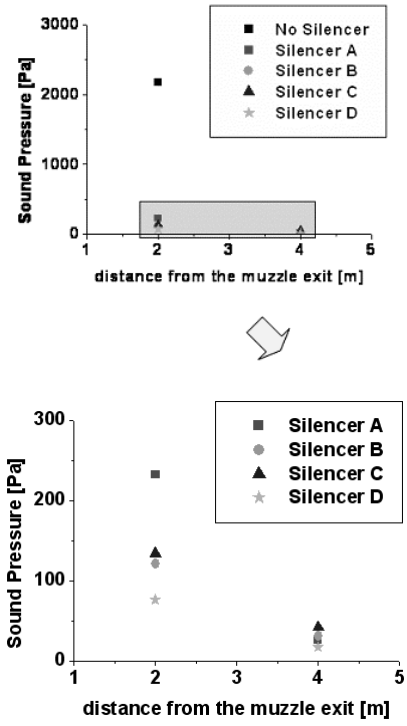

Fig. 17. Sound pressure from the gun muzzle.

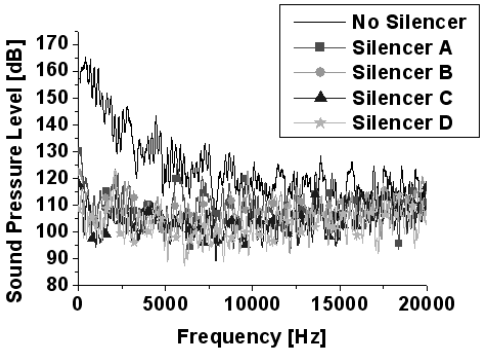

Fig. 18. Sound pressure level according to frequency ranges.

With silencer D, the sound pressure level reaches below 125 dB over all audible frequency ranges. Silencer D shows particularly excellent noise attenua tion at the high-frequency range of 15 to 20 kHz. It achieves a 40 dB reduction of sound pressure level at lower frequency ranges. It was found that silencer D efficiently attenuates impulsive noise over all audible frequency ranges.

Throughout this study, parameters for designing the silencer and for noise attenuation over the frequency ranges of 0 to 20 kHz were considered. The present data shows that in designing a gun silencer, the two parameters of baffle arrangement and location of the first baffle should be mainly considered. In order to further analyze silencer characteristics, further computational work was necessary (such as parametric studies and experimental work for various silencers). These results can be used for designing a silencer for LCWS.

5. Conclusions

These experimental and computational works have been carried out to study the complex high-pressure supersonic blast flowfield and impulsive sound attenuation. A numerical solver for analyzing high pressure supersonic blast flowfields has been developed. Through predicting the performance of the three-baffle silencer, a 42 dB attenuation of sound pressure level was investigated.

In the live firing test for the given silencers, a coniderable amount of propellant energy was dissipated in the chamber volume of the silencer and, as well, the sound pressure level was diminished. It was found that silencer D has good efficiency in attenuating impulsive noise over all audible frequency ranges. The present results show that the two parameters of baffle arrangement and location of the first baffle should mainly be considered for designing a gun silencer. The results of this study will be helpful for better understanding blast wave characteristics and for designing a silencer for LCWS.

References

[1] S. Pfüller, The management of shooting noise in german military training areas, Internoise 2003, The 32nd International Congress and Exposition on Noise Control Engineering. (2003).

[2] L. L. Pater and J. W. Shea, Techniques for reducing gun blast noise levels : An experimental study, NSWS TR 81-120 (1981).

[3] G. Helwolt, Review on noise abatement measures at military training facilities in germany, Internoise (1996) 1765-1768.

[4] C. H. Cooke and K. S. Fansler, Numerical simulation and modeling of a muffler, BRL-MR-3735. (1989).

[5] K. S. Fansler and R. von Wahlde, A muffler design for tank cannon acceptance testing BRL-MR-3931 (1991).

[6] Zonglin Jiang, Wave dynamic processes induced by a supersonic projectile discharging from a shock tube, *Physics of Fluids* 15 (6) (2003) 1665-1675.

[7] M. K. Hudson and C. Luchini, The evaluation of computational fluid dynamics methods for design of muzzle blast suppressors for firearms, *Propellants, Explosives, Pyrotechnics* 26 (2001) 201-208.

[8] J. C. T. Wang and G. F. Widhopf, Numerical simulation of blast flowdields using a high resolution TVD finite volume scheme, *Computers & Fluids* 18 (1) (1990) 103-137.